Solid State Ionics 181 (2010) 1258–1263

Contents lists available at ScienceDirect

Solid State Ionics

journal homepage: www.elsevier.com/locate/ssi

Proton conductivity in $Ln_{1.96}Ca_{0.04}Sn_2O_{7-\delta}$ (Ln = La, Sm, Yb) pyrochlores as a function of the lanthanide size

K.E.J. Eurenius, E. Ahlberg, C.S. Knee *

Department of Chemistry, University of Gothenburg, SE-412 96 Göteborg, Sweden

ARTICLE INFO

Article history:
Received 31 October 2009
Received in revised form 15 June 2010
Accepted 10 July 2010

Keywords:
Proton conductor
Lanthanide contraction
Pyrochlore
Electrochemical impedance spectroscopy
Infrared spectroscopy
Thermogravimetric analysis

ABSTRACT

The proton conductivity in tin-based pyrochlores, $Ln_{1.96}Ca_{0.04}Sn_2O_{7-\delta}$ (Ln = La, Sm, Yb), has been investigated. Samples were prepared by conventional solid state sintering methods. Fractions of the powders were vacuum dried, protonated and deuterated so that infrared spectroscopy and thermogravimetric analysis could be carried out to study proton incorporation. Electrochemical impedance spectroscopy was used to characterise the conductivities of the sample. The bulk conductivity was higher in wet gas compared to the dry runs at temperatures below approximately 500 °C for all samples. The level of proton conductivity was found to depend critically on the lanthanide size, and was highest for the largest La and mid-sized Sm ions, $\sigma_{H+} \approx 4 \times 10^{-7}$ Scm^{-1} at 300 °C, before falling sharply for the Yb-ion, $\sigma_{H+} \approx 7 \times 10^{-9}$ Scm^{-1}. Evidence from TGA and IR analyses indicates that the tendency for proton absorption was strongly influenced by the lanthanide size, being greatest for $La_{1.96}Ca_{0.04}Sn_2O_{7-\delta}$. The results suggest that both proton concentration and proton mobility vary depending on the size of the A-site ion.

1. Introduction

Proton conducting solid oxide fuel cells could play an important role in future power generation needs and this creates a strong interest in the development of new solid state electrolyte materials. The low activation energy of proton motion makes research into proton conducting electrolyte materials in the intermediate temperature range 200–600 °C an active research field [1–3]. Pyrochlore structured materials have been studied regarding structure, physical and electrical properties [4,5] but not to the same extent as for instance perovskites. However, ion conducting pyrochlores have been of significant interest as potential candidate materials in various parts of fuel cells, sensors for hydrogen and water or electrochemical reactors [6–9]. In particular the empty anion sites in the pyrochlore structure provide a possibility for high levels of oxide ion conductivity. Oxide ion conductivity may be enhanced via acceptor-doping the compounds with other ions of lower valence state than the host, on for example the A-site, to form additional oxide ion vacancies [10].

The proton conductivity of acceptor-doped $La_2Zr_2O_7$ pyrochlores has been extensively studied [11–13], and here the proton conductivities are seen to be ~1–2 orders of magnitude lower than the best performing perovskites in the intermediate temperature range. A number of studies showing a significant proton conductivity in pyrochlores with Ti at the B-site have also been reported [14–16]. The present authors have also studied the proton conduction properties of $Sm_2Sn_2O_7$ systems [17].

Here we present the results of an investigation of the proton conductivity of $Ln_{1.96}Ca_{0.04}Sn_2O_{7-\delta}$ (Ln = La, Sm, Yb) tin-based pyrochlores. The primary focus of the work was to resolve the impact of the lanthanide ionic size on the proton conductivity. As demonstrated for other proton conducting oxide structure-types, variation of the lanthanide size can strongly influence the level of proton incorporation, proton mobility and overall proton conduction [18,19]. Tin-based systems were selected as the ionic radius of tin unusually allows the stabilisation of the pyrochlore structure across the entire lanthanide series [20,21].

2. Experimental

Samples of $Ln_{1.96}Ca_{0.04}Sn_2O_{7-\delta}$ (Ln = La, Sm, Yb) were prepared via conventional solid state reactions of high purity reactants (La_2O_3 (99.9%), Sm_2O_3 (99.9%), Yb_2O_3 (99.9%), $CaCO_3$ (99.9%) and SnO_2 (99.9%)) as described in previous studies [16,17]. Acceptor-doping of all systems with the same amount of dopant was performed via partial substitution of La^{3+}, Sm^{3+} and Yb^{3+} for Ca^{2+}, to give the same nominal level oxygen vacancies, i.e. $\delta = 0.02$. Pellets were pressed (13 mm diameter) for electrochemical impedance spectroscopy runs. For IR and TGA analysis, small fractions of the as-prepared samples were hydrated in a humidifier (300 °C, 120 h) under a flow of nitrogen saturated with H_2O or D_2O at 74.4 °C ($p(H_2O) = 0.39$ atm.). Dried samples were prepared by annealing portions of the as-prepared samples at 1000 °C under vacuum (5×10^{-6} mbar, 12 h).

* Corresponding author. Tel.: +46 317863096.
E-mail address: knee@chem.gu.se (C.S. Knee).

0167-2738/$ – see front matter © 2010 Elsevier B.V. All rights reserved.
doi:10.1016/j.ssi.2010.07.001

To assess phase purity, XRD was carried out at room temperature using a Siemens D5000 powder diffractometer (Cu-K_α = 1.5418 Å, 25– 65° 2θ). High quality long scan data sets were collected with a Bruker D8 Advance instrument with a primary monochromator (Cu-$K_{\alpha1}$ = 1.54056 Å, 12–105° 2θ) and the data were analysed by the Rietveld method using the GSAS program [22] and initial structural models taken from [21].

The infrared (IR) absorbance spectra were obtained as in previous studies [16,17]. To collect high quality data, a Bruker IFS 66v/S vacuum Fourier transform IR interferometer was used with a KBr beam splitter and a mercury cadmium tellurium detector (560–6000 cm^{-1}). The system was flushed with dry CO_2-free air and spectra collected using a diffuse reflection unit. A reference spectrum diffused from ground KBr was measured before collecting each sample (400 scans/run). The spectra were then derived by taking the logarithm of the ratio between the reference spectrum and the sample spectrum.

TGA was preformed on vacuum dried, as-prepared and hydrated samples during heating (25–1000 °C, 15 °C/min) with a NETZSCH STA 409 PC, under a nominally dry flow of gas (N_2, 10 ml/min). Characterisation of the microstructure was carried out using a Leo Ultra 55 SEG SEM, operated with an acceleration potential of 3 kV and a secondary electron (SE) detector.

The impedance was measured between 4.5 MHz and 1 Hz with a Solatron 1260 frequency response analyser using a stand alone mode in a conductivity cell (ProboStat™) [23]. The sine wave amplitude was 1 V rms. In order to ensure a good ohmic contact, around 0.8 cm^2 of the pellets' surfaces were painted with Pt-paste (actual coverage was determined accurately using an Optic Zeiss 120 HD Microscope). Pt-grids were attached to the electrodes with Pt-wires. The relative densities recorded for the La-, Sm- and Yb-pellets were 82, 86 and 71% respectively. The runs were set to start heating from room temperature up to 1000 °C under a flow of Ar, which was passed over P_2O_5 to dry it or bubbled through H_2O or D_2O at RT to provide wet gas conditions ($p(H_2O)$ = 0.026 atm). The equilibration time was set to 30 min and data were collected on cooling in 50 °C intervals down to 150 °C. Further details of the measurement procedure can be found in references [16,17].

3. Results

The products obtained were off-white powders. Purity and the cubic crystal symmetry (Fd-3 m) were confirmed from the long scan XRD data (Fig. 1) and Rietveld refinements. The pattern of the La-containing material is shifted to lower 2θ-values, followed by the Sm-sample while the diffraction peaks of the Yb-system are found at higher angles. This indicates that the lattice parameter for the La-pyrochlore is larger than the Sm-containing sample and that the Yb-pyrochlore has the smallest cell parameter as expected due to the decreasing ionic radii of the 8-fold A-site ions, i.e., La: 1.16, Sm: 1.08 and Yb: 0.99 Å [24]. The cell parameters, along with other refined structural parameters obtained from Rietveld analyses, for the $(Ln_{1.96}Ca_{0.04})Sn_2O_{7-\delta}$ compounds are listed in Table 1. The cell constants compare to values of 10.7026(1), 10.51005(2) and 10.3046(1) Å reported by Kennedy et al. [21] for undoped $Ln_2Sn_2O_7$ samples. The small and systematic increase in cell parameter we observe may reflect the presence of Ca^{2+} (i.r. = 1.12 Å in 8-fold coordination) which has a larger ionic radius than Sm^{3+} [24].

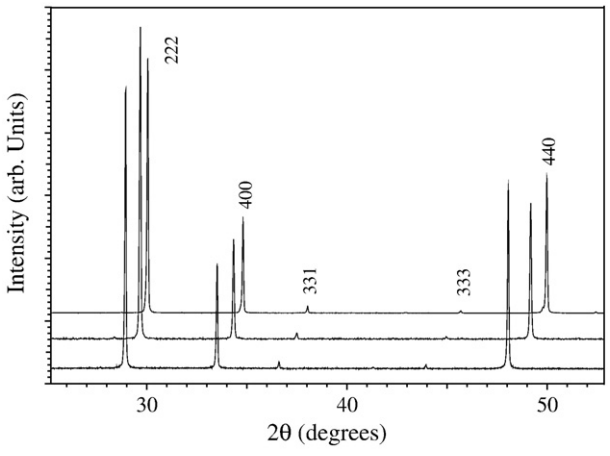

Fig. 1. XRD patterns for $Ln_{1.96}Ca_{0.04}Sn_2O_{7-\delta}$. The data shown are for Yb-, Sm- and La-samples from top to bottom. Miller indices for the most prominent pyrochlore reflections are labelled for the Yb-sample. The samples were sintered at 1500 °C as described previously [16].

The IR spectra for the hydrated, deuterated, as-prepared and vacuum dried samples are shown (Fig. 2) where significant variations between the hydrated and dried samples for all the samples are apparent. As expected, the hydrated and dried samples show the largest difference at ~3500 cm^{-1}. The peaks in this region are expected to be the O–H stretch vibrations and indicate dissolved protons in the hydrated compound, which are removed on annealing under vacuum. For $La_{1.96}Ca_{0.04}Sn_2O_{7-\delta}$ (Fig. 2a) the protonated and as-prepared samples are nearly identical suggesting that protonation occurs from atmospheric humidity on cooling from the synthesis temperature. For this sample three intense peaks at 3536 (labelled α), 3496 (β) and 3251 (γ) cm^{-1}, along with at least two other bands at 3420 and 3345 cm^{-1} are visible. Protonated $Sm_{1.96}Ca_{0.04}Sn_2O_{7-\delta}$ reveals a similar spectrum, with three intense bands at 3527, 3456 and 3311 cm^{-1} and two weaker peaks at 3422 and 3385 cm^{-1}. The deuterated La-and Sm-samples show new intensities in the region 2600–2300 cm^{-1}, and these peaks can be related to the O–H stretches through the expected ratio, i.e. $\upsilon_{OH}/\upsilon_{OD} \approx 1.37$, reflecting the change in the effective mass of the O–H and O–D groups. A feature of all the spectra recorded for the Sm-sample are the five peaks between ~2550 and 2200 cm^{-1} most clearly seen in the as-prepared and vacuum dried spectra. These peaks show no dependence on hydration history and are assigned as electronic transitions between the *f*-orbitals of the Sm^{3+} ion [25,26]. These features complicate somewhat the assignment of O–D stretches for the deuterated $Sm_{1.96}Ca_{0.04}Sn_2O_{7-\delta}$ sample (Fig. 2b). Nonetheless, enhancements of the intensity of the peaks at ~2550 and 2450 cm^{-1} coming from new O–D vibrations are apparent for the sample. Data for the deuterated Yb-sample revealed characteristic O–D stretches in the region 2600–2400 cm^{-1}, however, the results of the hydration runs for this material were not reliably reproducible and hence no IR data for $Yb_{1.96}Ca_{0.04}Sn_2O_{7-\delta}$ is presented.

TGA was carried out on hydrated, as-prepared and vacuum dried samples and selected results are shown in Fig. 3. Small but clear mass losses, with onset temperatures of ~400 °C, are apparent for the La- and Sm-based samples, while the Yb-compound showed a more gradual and less significant mass loss starting at a lower temperature ~200 °C, detectable from comparison of the traces obtained for the vacuum dried and protonated sample shown in Fig. 3. For the as-prepared $La_{1.96}Ca_{0.04}Sn_2O_{7-\delta}$ sample the TGA data was similar to the result obtained for

Table 1
Refined structural parameters for $Ln_{1.96}Ca_{0.04}Sn_2O_{7-\delta}$ pyrochlores.

	$La_{0.96}Ca_{0.04}$	$Sm_{1.96}Ca_{0.04}$	$Yb_{1.96}Ca_{0.04}$
a (Å)	10.7192(2)	10.5225(2)	10.3182(3)
x (x, 1/8, 1/8)	0.3270(20)	0.3360(21)	0.3388(21)
Isotropic thermal parameters ($Å^2$)			
Ln/Ca (0.5,0.5,0.5)	0.0042(10)	0.0198(15)	0.0127(13)
Sn (0,0,0)	0.0084(11)	0.0187(18)	0.0221(15)
O(1) (x, 1/8, 1/8)	0.025 [a]	0.025 [a]	0.025 [a]
O(2) (3/8,3/8,3/8)	0.025 [a]	0.025 [a]	0.025 [a]
R_{wp} (%)	16.01	7.52	12.68
R_p (%)	11.55	5.54	9.24
χ^2	2.343	1.42	1.98

[a] Note that the thermal parameters of the oxygen ions were not varied.